Mid-IR photoluminescence of Fe^{2+} and Cr^{2+} ions in ZnSe crystal under excitation in charge transfer bands

J. Peppers,* V. V. Fedorov, and S. B. Mirov

Center for Optical Sensors and Spectroscopies and the Department of Physics, University of Alabama at Birmingham, CH 310, 1300 University Blvd., Birmingham, Alabama 35294, USA
jpeppers@uab.edu

Abstract: Spectroscopic characterization of Fe:ZnSe(Cr:ZnSe) crystals under visible excitation into the charge transfer bands of Transition Metal ions were studied. The excitation efficiencies of mid-IR photoluminescence between $^5T_2(^5E)$ and $^5E(^5T_2)$ states via direct relaxation to the upper laser levels and via metastable upper $^3T_1$ were investigated. It was demonstrated that the latter route is the dominant process for Cr^{2+} ions and could provide sufficient pump rate for mid-IR lasing. The pump efficiencies via direct relaxation to the upper laser levels were estimated to be <2% for both ions under 532 nm excitation wavelength.

OCIS codes: (140.3070) Infrared and far-infrared lasers; (140.5680) Rare earth and transition metal solid-state lasers; (160.6990) Transition-metal-doped materials.

References and links

1. S. Mirov, V. Fedorov, D. Martyshkin, I. Moskalev, M. Mirov, and S. Vasilyev, "Progress in mid-IR lasers based on Cr and Fe doped II-VI chalcogenides," IEEE J. Sel. Top. Quantum Electron. **21**(1), 1601719 (2015).
2. S. B. Mirov, V. V. Fedorov, D. V. Martyshkin, I. S. Moskalev, M. S. Mirov, and V. P. Gapontsev, "Progress in mid-IR Cr^{2+} and Fe^{2+} doped II-VI materials and lasers [Invited]," Opt. Mater. Express **1**(5), 898–910 (2011).
3. S. Mirov, V. Fedorov, I. S. Moskalev, D. Martyshkin, and C. Kim, "Progress in Cr^{2+} and Fe^{2+} doped mid-IR laser materials," Laser Photonics Rev. **4**(1), 21–41 (2010).
4. V. I. Kozlovsky, V. A. Akimov, M. P. Frolov, Yu. V. Korostelin, A. I. Landman, V. P. Martovitsky, V. V. Mislavskii, Y. P. Podmar'kov, Y. K. Skasyrsky, and A. A. Voronov, "Room-temperature tunable mid-infrared lasers on transition-metal doped II–VI compound crystals grown from vapor phase," Phys. Status Solidi B **247**(6), 1553–1556 (2010).
5. N. Myoung, D. V. Martyshkin, V. V. Fedorov, and S. B. Mirov, "Mid-IR lasing of iron–cobalt co-doped ZnS(Se) crystals via Co–Fe energy transfer," J. Lumin. **133**, 257–261 (2013).
6. J. Peppers, N. Myoung, V. V. Fedorov, and S. B. Mirov, "Mid-IR laser oscillation via energy transfer in the Co:Fe:ZnS/Se co-doped crystals," Proc. SPIE **8235**, 823503 (2012).
7. V. V. Fedorov, A. Gallian, I. Moskalev, and S. B. Mirov, "En route to electrically pumped broadly tunable middle infrared lasers based on transition metal doped II–VI semiconductors," J. Lumin. **125**(1–2), 184–195 (2007).
8. C. I. Rablau, "Photoluminescence and optical absorption spectroscopy of infrared materials Cr^{2+}:Znse and $ZnGeP_2$," Ph.D. dissertation, West Virginia University, Morgantown, West Virginia (1999).
9. M. Surma, A. J. Zakrzewski, and M. Godlewski, "Nonradiative recombination processes in nickel- and iron-doped ZnS and ZnSe studied by photoinduced electron-spin resonance," Phys. Rev. B Condens. Matter **52**(16), 11879–11883 (1995).
10. V. Yu. Ivanov, Y. G. Semenov, M. Surma, and M. Godlewski, "Anti-Stokes luminescence in chromium-doped ZnSe," Phys. Rev. B Condens. Matter **54**(7), 4696–4701 (1996).
11. M. Godlewski, "On the application of the photo-EPR technique to the studies of photoionization, DAP recombination, and non-radiative recombination processes," Phys. Status Solidi A **90**(1), 11–52 (1985).
12. J. Kreissl and H.-J. Schulz, "Transition-metal impurities in II-VI semiconductors: characterization and switching of charge states," J. Cryst. Growth **161**(1–4), 239–249 (1996).
13. M. Godlewski and M. Skowronski, "Effective deactivation of the ZnS visible photoluminescence by iron impurities," Phys. Rev. B Condens. Matter **32**(6), 4007–4013 (1985).
14. V. V. Fedorov, T. Konak, J. Dashdorj, M. E. Zvanut, and S. B. Mirov, "Optical and EPR spectroscopy of Zn:Cr:ZnSe and Zn:Fe:ZnSe crystals," Opt. Mater. **37**, 262–266 (2014).

#230884 - $15.00 USD Received 18 Dec 2014; revised 23 Jan 2015; accepted 24 Jan 2015; published 12 Feb 2015

15. N. Myoung, V. V. Fedorov, S. B. Mirov, and L. E. Wenger, "Temperature and concentration quenching of mid-IR photoluminescence in iron doped ZnSe and ZnS laser crystals," J. Lumin. **132**(3), 600–606 (2012).
16. A. Burger, K. Chattopadhyay, J. O. Ndap, X. Ma, S. H. Morgan, C. I. Rablau, C. H. Su, S. Feth, R. H. Page, K. I. Schaffers, and S. A. Payne, "Preparation conditions of chromium doped ZnSe and their infrared luminescence properties," J. Cryst. Growth **225**(2-4), 249–256 (2001).
17. M. Skowronski, Z. Liro, and W. Palosz, "Uniaxial stress effect on no-phonon lines of $^3T_1$ to ^5E transitions in ZnS:Fe," J. Phys. Chem. **18**(26), 5099–5110 (1985).
18. K. P. O'Donnell, K. M. Lee, and G. D. Watkins, "An ODMR study of a luminescence excitation process in ZnSe:Fe," J. Phys. Chem. **16**(20), L723 (1983).
19. A. Zakrzewski and M. Godlewski, "Direct evidence of three-center-Auger recombination processes in ZnS:Cu,Fe," Phys. Rev. B Condens. Matter **34**(12), 8993–8995 (1986).
20. K. Swiatek, M. Godlewski, and T. P. Surkova, "Fe photoionization transitions in ZnSSe:Fe crystals – photo-ESR studies," Phys. Status Solidi C **2**(3), 1224–1227 (2005).
21. F. Träger, *Springer Handbook of Lasers and Optics*, (Springer Science + Business Media, 2007).
22. S. Kück, "Laser-related spectroscopy of ion-doped crystals for tunable solid-state lasers," Appl. Phys. B **72**(5), 515–562 (2001).
23. C. I. Rablau, J. O. Ndap, X. Ma, A. Burger, and N. C. Giles, "Absorption and photoluminescence spectroscopy of diffusion-doped ZnSe:Cr^{2+}," J. Electron. Mater. **28**(6), 678–682 (1999).
24. M. U. Lehr, B. Litzenburger, J. Kreiss, U. W. Pohl, H. R. Selber, H.-J. Schulz, A. Klimakow, and L. Worschech, "Identification of near-infrared Cr^{2+} luminescence in ZnSe," J. Phys. Condens. Matter **9**(3), 753–763 (1997).
25. V. Yu. Ivanov, M. Godlewski, and T. Gregorkiewicz, "Two-colour spectroscopy of ZnSe:Cr," Phys. Status Solidi B **244**(5), 1618–1622 (2007).
26. G. Grebe, G. Roussos, and H.-J. Schulz, "Cr^{2+} excitation levels in ZnSe and ZnS," J. Phys. Chem. **9**(24), 4511–4516 (1976).

1. Introduction

Tunable middle infrared (mid-IR) lasers are promising for a broad range of applications such as medical diagnosis, remote sensing, and optical communication. Within this class of lasers, the transition metal (TM) doped (e.g. chromium and iron) II-VI (e.g. ZnSe and ZnS) crystals are arguably gain media of choice for the development of broadly tunable laser systems operating at room temperature (RT) over the 2-6 μm spectral range [1–4].

Cr^{2+}:II-VI lasing has been demonstrated at room temperature in all regimes of operation with tunability over 1.9-3.3 μm range. Continuous wave (CW) output powers exceeding 30W and pulse energies of 1.1 J for free running and 50 mJ for gain-switched operation have been achieved [1]. This was made possible due to favorable spectroscopic characteristics. The tetrahedral crystal field of the II-VI hosts splits the ground level (^5D) of Cr^{2+} into the triplet $^5T_2$ and doublet ^5E level. Transitions between these levels are symmetry allowed while transitions to higher lying levels are spin forbidden, resulting in strong gain without excited state absorption. Additionally, while there is some quenching of the lifetime at room temperature, the lifetime remains at the level of several μs and is sufficient to obtain lasing in the CW operational regime. Fe^{2+}:II-VI also exhibits no excited state absorption and lasing has been demonstrated in all regimes of operation over the 3.5-6 μm spectral range with CW power of 1.6 W and pulse energies 2.1 J in free running, and 30 mJ in the gain-switched regime [1]. However, the strong quenching of Fe^{2+} lifetime at room temperature requires cryogenic systems to operate in all regimes except gain-switching, which has been demonstrated at room temperature.

The current prevailing excitation method for these lasers is intra-band optical excitation in the broad absorption bands of Cr^{2+} and Fe^{2+} ions centered at 1.8 μm and 3 μm, respectively. This enables a set of available pump sources in the case of Cr^{2+} (Er, Tm, Ho lasers) and only a few for Fe^{2+}. Our recent work has been directed at extending the range of available avenues of excitation for these ions and we have demonstrated lasing with low pulse energy in Co:Fe:ZnSe and Co:Fe:ZnS through $Co^{2+} \rightarrow Fe^{2+}$ energy transfer [5,6].

The focus of the current research is to extend the available pump source through the study of the relaxation of TM^{2+} ions subsequent to excitation into the charge transfer band. The introduction of chromium or iron into the lattice of ZnSe or ZnS wide bandgap semiconductors is accompanied by the formation of a charge transfer band in the bandgap.

#230884 - $15.00 USD Received 18 Dec 2014; revised 23 Jan 2015; accepted 24 Jan 2015; published 12 Feb 2015

This results in strong visible absorption at wavelengths just above those corresponding to photon energies of 2.7 and 3.5 eV for ZnS and ZnSe, respectively. Previously, charge transfer processes of iron and chromium doped ZnSe/ZnS were studied using EPR and spectroscopic methods [7–14]. An understanding of the relaxation process under visible excitation in Cr^{2+} and Fe^{2+} ZnSe/ZnS crystals cannot only provide an alternative pumping method in the form of optical excitation, but also a better understanding of processes that could lead to the development of a new type of solid-state lasers with electrical pumping.

2. Experimental details

The polycrystalline samples utilized in these experiments were produced by thermal diffusion of transition metal ions into bulk II-VI hosts. A thin film of chromium or iron was deposited on the surface of ZnSe optical windows, which were then sealed in quartz ampoules under vacuum (~10^{-5} Torr) and annealed in a furnace at high temperature for several days to promote thermal diffusion from the facets to the crystal volume. The annealing temperature and exposure time have been carefully adjusted for each dopant to provide minimal distribution gradient while maintaining high crystal quality. Three samples were examined in this study. One low concentration Cr:ZnSe (N_{Cr} = 2.7 × 10^{18} cm^{-3}) was used only for absorption measurements. All other experiments were carried out with Fe:ZnSe and Cr:ZnSe samples with concentrations typical for use as gain elements (N_{Fe} = 1.4 × 10^{19} cm^{-3} and N_{Cr} = 8.2 × 10^{18} cm^{-3} respectively). The concentration dependence of the photoluminescence (PL) in Cr:ZnSe and Fe:ZnSe were previously reported [15,16]. These studies demonstrated concentration quenching of the RT PL in Cr doped samples with concentration higher than 10^{19} cm^{-3} [16]. In iron doped samples the nonradiative relaxation processes at RT are more pronounced in comparison with chromium doped samples and the influence of iron concentration becomes apparent for concentrations larger than 5 × 10^{19} cm^{-3} [15] (see [15,16] for more detail). In our experiments we focused our study on samples with TM concentrations usually used for mid-IR laser oscillation.

The absorption spectra were measured at room temperature using Shimadzu UV-VIS-NIR-3101PC and FTIR spectrophotometers.

The excitation sources used for photoluminescence spectra and kinetics measurements were a Spectra-Physics Quanta-Ray Nd:YAG laser and MOPO system as well as an electro-optically Q-switched Cr:Er:YSGG laser.

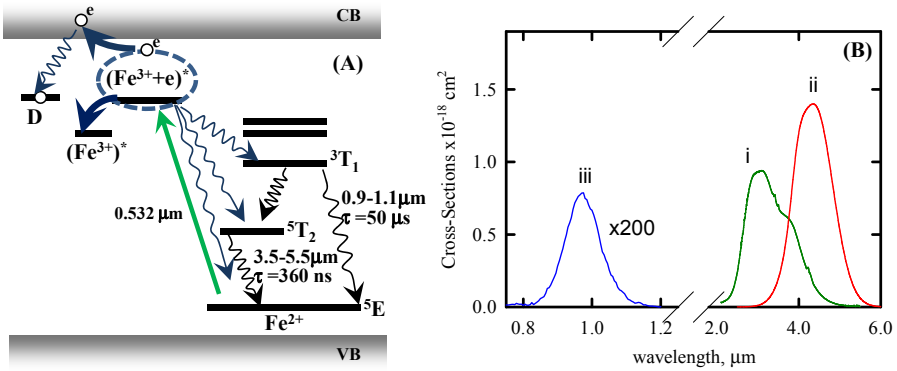

Fig. 1. A. Energy levels of Fe^{2+} and energy transfer mechanisms. B. Cross-sections of near-IR and mid-IR transitions in Fe:ZnSe.

Emission spectra were obtained by collecting PL radiation with a CaF_2 lens and directing into a monochromator, with the signal detected by either Thorlabs PDA20H PbSe detector (λ = 1.5-4.8 µm) or photomultiplier tube (λ<1.2 µm) and signal processing performed with the aid of a Stanford Research Systems boxcar integrator and Acton Research Corporation

#230884 - $15.00 USD Received 18 Dec 2014; revised 23 Jan 2015; accepted 24 Jan 2015; published 12 Feb 2015

spectral measurement system. PL kinetics were measured using three detectors; liquid nitrogen cooled InSb detector, VIGO Systems PVI-3TE-6 (HgCdTe) detector sensitive over the 2-12 μm range with response time < 200 ns, and Hamamatsu R406 Ag-O-Cs photomultiplier tube with sensitivity over the 0.4-1.1 μm range and 2 ns rise time for near infrared. Spectra were adjusted for detector sensitivity using Newport 6575 (mid-IR) and Oriel 63358 (near-IR) calibration lamps.

3. Experimental results and discussions

3.1 Fe:ZnSe samples

Energy level structure of the $Fe^{2+}(3d^6)$ is shown in Fig. 1(a). The ^5D ground states of the Fe^{2+} in the tetrahedral crystal field (Td) of ZnSe crystal are split into the doublet ^5E (ground state) and triplet $^5T_2$, (first excited state), respectively. The absorption and emission bands at the laser active $^5E \leftrightarrow {}^5T_2$ transition in Fe:ZnSe crystals are shown in Fig. 1(b). As one can see, the RT absorption and emission spectra of Fe^{2+} reveal broad bands between 2.5 and 4.0 μm and 3.5-5.0 μm, respectively. The RT luminescence lifetime was measured to be 380 ns, while radiative lifetime at this transition was estimated at τ_{rad} = 57 μs [15]. The short upper level life-time applies restrictions on the excitation rate for laser application. That is why these crystals could efficiently oscillate in gain-switched regime at RT, but require cooling for effective CW lasing. The remaining transitions from ^5D sub-levels are spin forbidden. Near IR emission and absorption bands around ~1μm were attributed to the $^5E(^5D) \leftrightarrow {}^3T_1$ (^3H) transition of the Fe^{2+} ions in the II-VI semiconductors [13,17,18].

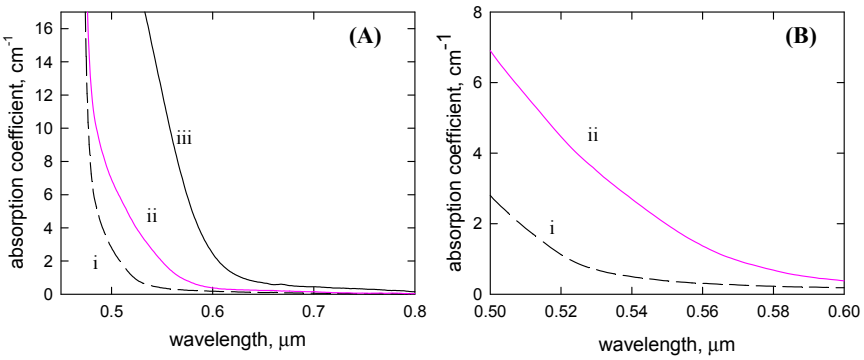

Fig. 2. A. Absorption spectra of undoped (i), iron doped (ii), and chromium doped (iii) ZnSe (N_{Fe} = 1.4 × 10^{19} cm^{-3}, N_{Cr} = 2.7 × 10^{18} cm^{-3}) crystals near band-gap, B. Zoom-in to show absorption of Fe:ZnSe near 532 nm.

As mentioned in the introduction, one of the research goals was to study the dynamics of excitation of the upper laser level ($^5T_2(^5D)$) under excitation into the charge transfer band in Fe:ZnSe crystals. Figure 2 shows absorption of the undoped ZnSe crystal and Fe:ZnSe crystal with iron concentration N_{Fe} = 1.4 × 10^{19} cm^{-3} in the visible spectral range. As one can see from the Fig. 2, the absorption coefficient in the charge transfer band near 532nm is ~4 cm^{-1}. This absorption coefficient is ~3 times smaller than for the direct excitation at $^5E \leftrightarrow {}^5T_2$ transition for the same crystal; however this value is sufficient for efficient absorption for longitudinal laser pumping.

There are several relaxation processes which could populate the upper laser level after excitation into charge transfer band (see Fig. 1(a)). The fastest process is direct non-radiative relaxation from the excited complex (Fe^{3+} + e)* to the upper laser level $^3T_2$ (^5D) [13]. This relaxation process should be very fast (~10-100 ps) in comparison with upper level life time (380 ns). The second excitation route could involve cascade relaxation through higher levels of Fe^{2+} ions. The bottleneck for these relaxation processes could be long lifetime of meta-

#230884 - $15.00 USD Received 18 Dec 2014; revised 23 Jan 2015; accepted 24 Jan 2015; published 12 Feb 2015

stable levels. The likely candidate for this bottleneck level is the $^3T_1(^3H)$ state. In this case, the relaxation time could vary from μs to ms time scale resulting in a process that is too slow to provide effective inversion population at $^3T_2$ (^5D) level. Finally, the slowest process could result from ionization of Fe^{2+} ions. In this case the electron excited to the conduction band is localized at the shallow donor (or donor-accepter pair). These ionization processes were thoroughly studied using EPR [13,19]. The variation of the distances between iron ions and shallow donor (or donor-acceptor pair) results in a significant decrease of the relaxation rate. For example, Auger type recombination for the $Cr^{1+} \rightarrow Cr^{2+}$ process in ZnSe crystals featuring characteristic non exponential decay with time constant of 12 sec at 78K was discussed in [14] and the decay of the EPR signal Fe^{3+} has been measured to be longer than tens of seconds at 100K in [20].

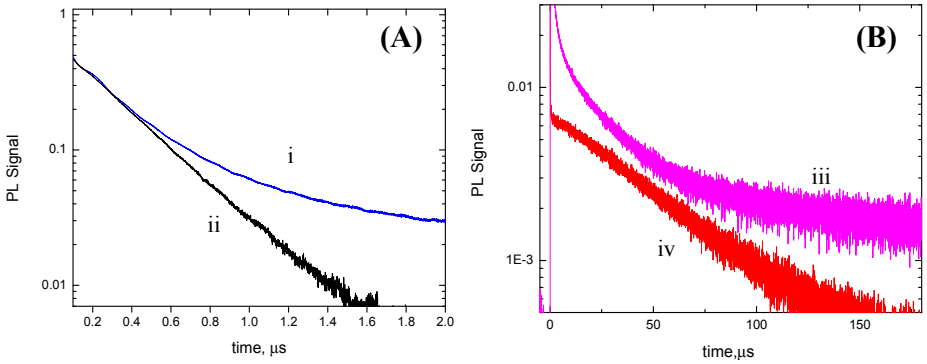

Fig. 3. A. Short PL kinetics of Fe:ZnSe under i) 532nm excitation and ii) 2780nm excitation. B. Long PL kinetics of Fe:ZnSe showing iii) mid-IR kinetics under 532nm excitation and iv) near-IR PL at 950nm.

To study the possible excitation mechanisms of the upper laser level we measured near IR and mid-IR kinetics of the photo-luminescence under direct excitation and excitation into the charge transfer band. Figure 3(a) shows decay of the mid-IR PL at $^5T_2 \rightarrow ^5E$ transition in Fe:ZnSe crystal at RT under 2.78 μm (curve ii) and 0.532 μm (curve i) excitation. In our experiments with detector response time of ~40 ns we did not measure any slow rise-time of the mid-IR PL under green excitation. This is indicative of fast non-radiative relaxation from the excited complexes $(Fe^{3+} + e)^*$ to the upper laser level $^5T_2$. Additional evidence for this process is also the fact that initial decay rates of the mid-IR signal under visible and direct excitation coincide. However, decay of the mid-IR PL signal reveals essentially non-exponential behavior. The curve (iii) in Fig. 3(b) shows the decay of the PL over long time-scale. For comparison, the near-IR PL at 950 nm with decay time 49 μs is also depicted in the Fig. 3(b) (curve iv). As one can see from the Fig. 3(b) the decay tail of PL signal under green excitation at ~100 μs time scale could result from cascade relaxation via $^3T_1$ level. Additional evidence for this relaxation channel is documented in the literature luminescence signal ~1.4 μm at low temperature associated with the $^3T_1(^3H) \rightarrow ^5T_2(^5D)$ transition [18]. However, as one can see from Fig. 3(b), there is an excitation channel with characteristic time which is longer than the lifetime of $^3T_1(^3H)$ level. This channel could be attributed to ionization transitions of iron ions. To estimate radiatave lifetime of the $^3T_1(^3H) \rightarrow ^5T_2(^5D)$ transition we measured kinetic at 970 nm at T = 20K. The exponential decay time was measured to be 390 μs. The maximum cross-section can be estimated using the formula of McCumber [21,22]:

$$\sigma_{max} = \sqrt{\frac{\ln 2}{\pi}} \frac{A}{4\pi c n^2} \frac{\lambda_0^4}{\Delta\lambda} \qquad (1)$$

#230884 - $15.00 USD Received 18 Dec 2014; revised 23 Jan 2015; accepted 24 Jan 2015; published 12 Feb 2015

Where λ_0 is the peak emission wavelength, $\Delta\lambda$ is the full width at half maximum, n is the refractive index, $A = 1/\tau$ is Einstein's coefficient of spontaneous emission for radiative lifetime τ. We estimated the maximum RT emission cross-section of the $^3T_1(^3H) \rightarrow {}^5T_2(^5D)$ transition to be 0.4×10^{-20} cm^2 (see Fig. 1(b)).

To estimate pump energy required for mid-IR lasing under green excitation we compared the PL signal under green and direct mid-IR excitation under the same experimental conditions and normalized PL signal to the absorbed energy. The total number of the excited ions is proportional to area under PL decay curve. However, for lasing excitation, only fast excitation rate (during time scale $< \tau = 380$ ns) could provide effective population at upper laser level. Therefore, one must compare area under the kinetics during the 380 ns period after excitation. We mentioned previously that initial decay rate under green excitation and under direct mid-IR excitation is similar, and area under these curves will be proportional to the signal amplitudes. In our experiments, the PL signal with amplitude 147 mV was measured under 50μJ of absorbed energy at 2.78 μm; while the PL signal with amplitude 27 mV was measured under 1.7mJ of absorbed energy at 0.53 μm. From these data, the estimated pump energy for green excitation should be approximately 185 times larger under the same geometry and direct excitation.

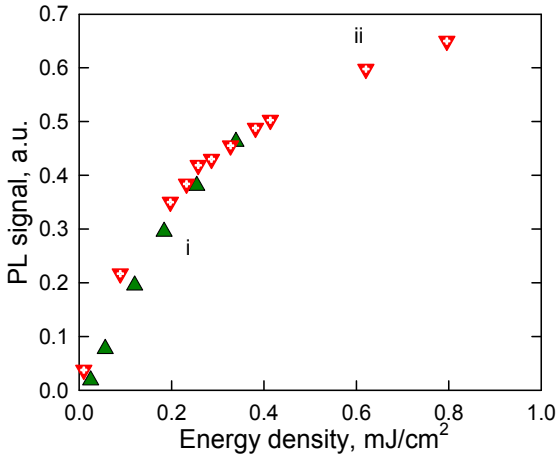

Fig. 4. Dependence of PL signal on energy of excitation for i) Fe:ZnSe and ii) Cr:ZnSe.

Figure 4 depicts dependence of the mid-IR PL signal on pump energy density. Deviation from linear dependence was observed under high energy density excitation. The nonlinear behavior indicates existence of two-photon or two-step processes which can result in reduction of the excitation efficiency. To summarize the observations pertaining to Fe:ZnSe, we see that in spite of the fast relaxation rate for the excitation of the $^5T_2$ level of Fe^{2+} ions under excitation into charge transfer band, the efficiency of this excitation is ~2% from absorbed photons. Considering that the RT laser threshold of Fe:ZnSe in the gain switched regime was demonstrated at ~1mJ, the estimated laser threshold under green excitation could be as much as 200 mJ. This could potentially be realized by using longer gain elements or multiple crystals in a cavity to reach laser threshold while avoiding optical damage.

#230884 - $15.00 USD Received 18 Dec 2014; revised 23 Jan 2015; accepted 24 Jan 2015; published 12 Feb 2015

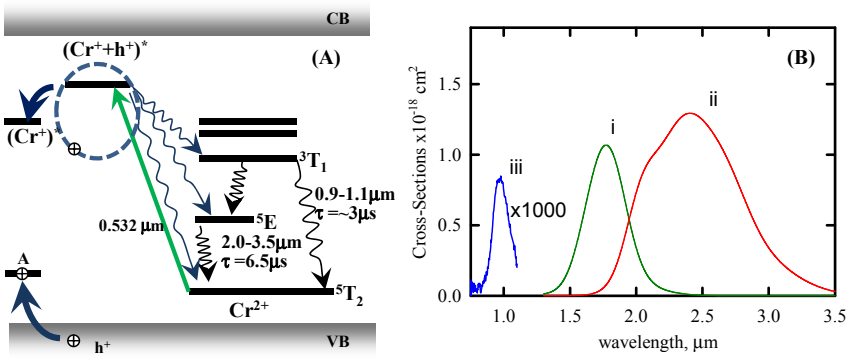

Fig. 5. A. Energy levels of Cr^{2+} and energy transfer mechanisms. B. Cross-sections of near-IR and mid-IR transitions in Cr:ZnSe

3.2 Cr:ZnSe samples

$Cr^{2+}(3d^4)$ ions have similar energy structure to Fe^{2+} ions, however the triplet $^3T_2$ is the ground level and the doublet ^5E is the first existed state level (see Fig. 5(a)). The laser transition between these levels is shifted to shorter wavelengths between 2 and 3.3 μm. Also the luminescence yield is 100% at RT with radiative lifetime 6.5 μs. The Cr^{2+} ions reveal stronger charge transfer band in comparison with Fe^{2+} ions (see Fig. 2(a)). The absorption coefficient at 590 nm has the same value as the maximum absorption coefficient under direct excitation at laser transitions between $^3T_2$ and ^5E levels. The high absorption cross section at 532 nm compared with mid-IR emission cross section necessitates transverse pump geometry.

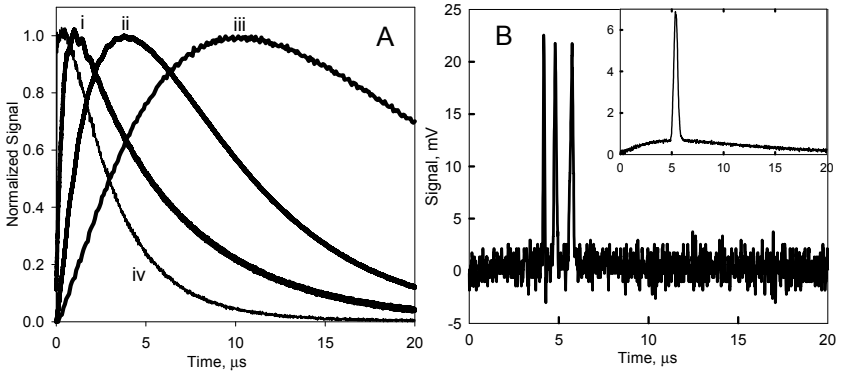

Fig. 6. A. Normalized PL kinetics of Cr:ZnSe illustrating rise time under i) intra-shell excitation at 1560nm, ii) 532nm nanosecond scale excitation, iii) 532nm picosecond scale excitation, and iv) Cr:ZnSe PL kinetics at 960nm under 532nm ns scale excitation. B. Lasing of Cr:ZnSe under 532nm 10ns pulsed excitation showing three pulses under 9.1mJ pump energy, with insert showing the averaged signal under 6.7mJ pump energy.

In our experiments we studied kinetics of the PL signal in Cr:ZnSe under 532 nm excitation at $^3T_1 \rightarrow {}^5T_2$ and $^5E \rightarrow {}^5T_2$ transitions. The measured RT near-IR PL band at the $^3T_1 \rightarrow {}^5T_2$ transition is similar to that in Fe:ZnSe between 880 and 1040 nm [23–26]. However, the measured RT kinetics at 950 nm reveals single exponential decay with lifetime τ = 2.8 μs. We also observed rise time behavior with maximum signal ~500 ns after excitation pulse which could be explained by cascade relaxation from a higher-lying level to the $^3T_1$ level. The radiative lifetime of the $^3T_1 \rightarrow {}^5T_2$ transition was estimated using the decay time of the near-IR PL kinetics at low temperature (20K) of 1.7 ms. Using the formula of McCumber [21,22] we estimated the maximum RT emission cross-section of the $^3T_1(^3H) \rightarrow {}^5T_2(^5D)$ transition to be

#230884 - $15.00 USD Received 18 Dec 2014; revised 23 Jan 2015; accepted 24 Jan 2015; published 12 Feb 2015

0.8×10^{-21} cm^2 (see Fig. 5(b)). It is important to note that these results show that at room temperature the $^3T_1$ level is quenched and the lifetime of the $^3T_1$ (2.8 μs) level is shorter than that of the upper laser level ^5E (6.5 μs). It is for this reason that the excitation route through $^3T_1$ could be used for laser excitation.

Intra-shell excitation of Cr:ZnSe by 1560nm radiation results in short rise time of mid-IR PL kinetics with measurement limited by the sensitivity of the detection system followed by exponential decay with lifetime ~6μs. Excitation into the charge transfer band is followed by a delay in mid-IR PL kinetics rise time with the peak occurring at several μs after excitation. 532nm nanosecond scale pulsed excitation results in rise time in the PL kinetics of ~3.5 μs. This rise time is very close to the life-time of the $^3T_1$ level. This suggests that the dominant excitation process to the ^5E level involves cascade relaxation from higher excited levels. The fast components of the direct excitation of the ^5E level could be seen only at low temperature when transition from $^3T_1$ level is "frozen". The efficiency of the fast excitation processes in comparison with relaxations via $^3T_1$ level could be estimated by comparing the area under the fast and slow component of mid-IR kinetics. Calculations show that at low temperature excitation via $^3T_1$ level is responsible for 98% of ^5E level inversion under green excitation.

The dependence of the PL signal on pump energy density is shown in Fig. 4 (curve ii). The decrease of the excitation efficiency is clearly seen for energy density >0.2 mJ/cm^2. The efficiency of excitation differs greatly with intensity of the 532nm pump, with ~100% efficiency measured under CW excitation and ~14% quantum efficiency measured under 10ns pulsed excitation with energy density of 7.7mJ/cm^2. As previously stated, the higher peak power of pump pulses can enable additional channels for absorption of pump radiation such as two-step (Eq. (2)) or two-photon (Eq. (3)) processes:

$$Cr^{2+} + \hbar\omega \rightarrow Cr^{+} + h^{+} \text{ followed by } Cr^{+} + \hbar\omega \rightarrow (Cr^{2+})^{*} + e^{-}, \text{ or} \quad (2)$$

$$Cr^{2+} + 2\hbar\omega \rightarrow (Cr^{+})^{*} + (h^{+})^{*} \quad (3)$$

where h^+ denotes a positive charge carrier (hole), e^- an electron, Cr^{2+} and Cr^+ are ionization states of chromium. The asterisk (e.g. $(Cr^{2+})^*$ and $(Cr^+)^*$) denotes highly excited states.

The observed increase of the rise time of the mid-IR kinetics from 3.5 μs to ~10 μs delay measured under excitation by 35 ps pulses at 532 nm excitation (see Fig. 6 curve iii) in comparison with ns excitation could be explained by including slow relaxation processes under high power excitation.

The quenching of the $^3T_1$ level to the value below lifetime of the ^5E level at RT allows the use of this excitation route for laser applications. Cr:ZnSe lasing experiments were performed with transverse pumping geometry in an optical cavity composed of a gold back mirror with 5cm radius of curvature and a planar output coupler. The 532 nm radiation was focused into a line along the cavity axis with a cylindrical lens. The crystal used was 8.5mm long with chromium concentration of 8.2×10^{18} cm^{-3} and AR coated at laser wavelength. The results of these lasing experiments are shown in Fig. 6(b). Three laser pulses are visible in the kinetics beginning ~4μs after excitation, which are the result of slow accumulation of population in the upper laser level after excitation to higher lying levels. When this population reaches threshold, lasing depletes the population quickly allowing subsequent repopulation and lasing. This long timescale repopulation of the upper laser level produces pulse trains similar to free running. The graph insert in Fig. 6(b) shows lasing slightly above threshold to illustrate the timing of the lasing spike relative to the luminescence. The lasing was confirmed by shortening of the kinetics behavior and narrowing of the measured spectra. Unfortunately, the laser threshold was very close to the optical damage threshold of the Cr:ZnSe crystal, precluding measurement of the input-output characteristics.

#230884 - $15.00 USD Received 18 Dec 2014; revised 23 Jan 2015; accepted 24 Jan 2015; published 12 Feb 2015

4. Conclusions

Analysis of the mid IR luminescence of Fe^{2+} and Cr^{2+} ions in ZnSe under visible excitation allowed estimation of the excitation efficiency of the upper laser level. The near-IR emission cross sections from $^3T_1$ levels were estimated to be 0.8×10^{-21} cm^2 and 0.4×10^{-20} cm^2 at RT for Cr^{2+} and Fe^{2+} ions, correspondingly. The efficiency of the fast non-radiative relaxation to the upper laser level for both ions was estimated to be not more than ~2% from absorbed energy of ns excitation pulses. However in Cr^{2+} ions the cascade relaxation over $^3T_1$ level exhibits lifetime of 2.8 μs which is shorter than that of the upper laser level (6.5 μs) and could therefore provide pumping rate sufficient for laser operation. The similar excitation route for Fe^{2+} ions has relaxation time ~50 μs which is significantly longer than the lifetime of the upper level at RT (380 ns). This results in an estimated pump threshold under 532nm excitation of 185 times that of 2.78μm excitation, making this excitation method more susceptible to optical damage. One way to potentially increase efficiency of pumping under visible excitation would be the utilization of cross-relaxation processes in highly doped crystals, which is a subject for future investigation.

Acknowledgments

The authors would like to acknowledge funding support from the AF Office of Scientific Research (Award No. FA9550-13-1-0234), and the National Science Foundation under grant EPS-0814103. The work reported here partially involves intellectual property developed at the University of Alabama at Birmingham (UAB). This intellectual property has been licensed to the IPG Photonics Corporation. Drs. Fedorov and Mirov declare competing financial interests.

#230884 - $15.00 USD Received 18 Dec 2014; revised 23 Jan 2015; accepted 24 Jan 2015; published 12 Feb 2015